Research Article | Vol. 25, No. 17 | 21 Aug 2017 | OPTICS EXPRESS 19711
Optics EXPRESS

Silicon photonic filters with high rejection of both TE and TM modes for on-chip four wave mixing applications

GIUSEPPE CANTARELLA,[1] CHARALAMBOS KLITIS,[2] MARC SOREL,[2] AND MICHAEL J. STRAIN[1,*]

[1] *Institute of Photonics, Dept. of Physics, University of Strathclyde, Glasgow, G1 1RD, UK*
[2] *School of Engineering, University of Glasgow, Glasgow, G12 8LT, UK*
[*] *michael.strain@strath.ac.uk*

Abstract: Wavelength selective filters represent one of the key elements for photonic integrated circuits (PIC) and many of their applications in linear and non-linear optics. In devices optimised for single polarisation operation, cross-polarisation scattering can significantly limit the achievable filter rejection. An on-chip filter consisting of elements to filter both TE and TM polarisations is demonstrated, based on a cascaded ring resonator geometry, which exhibits a high total optical rejection of over 60 dB. Monolithic integration of a cascaded ring filter with a four-wave mixing micro-ring device is also experimentally demonstrated with a FWM efficiency of -22dB and pump filter extinction of 62dB.

© 2017 Optical Society of America

OCIS codes: (130.3120) Integrated optics devices; (130.4310) Nonlinear; (130.7408) Wavelength filtering devices; (130.3990) Micro-optical devices; (130.7405) Wavelength conversion devices.

References and links

1. R. Soref, "The past, present, and future of silicon photonics," IEEE J. Sel. Top. Quantum Electron. **12**, 1678–1687 (2006).
2. V. R. Almeida, C. A. Barrios, R. R. Panepucci, and M. Lipson, "All-optical control of light on a silicon chip," Nature **431**, 1081–1084 (2004).
3. L. C. Kimerling, "Silicon microphotonics," Appl. Surf. Sci. **159**, 8–13 (2000).
4. G.T. Reed, A.P. Knights, *Silicon Photonics: an Introduction,* (John Wiley & Sons, 2004).
5. W. Bogaerts, R. Baets, P. Dumon, V. Wiaux, S. Beckx, D. Taillaert, B. Luyssaert, J. Van Campenhout, P. Bienstman, and D. Van Thourhout, "Nanophotonic waveguides in silicon-on-insulator fabricated with CMOS technology," IEEE J. Lightwave Technol. **23**, 401–412 (2005).
6. C. Gunn, "CMOS Photonics for High-Speed Interconnects," IEEE Micro **26**, 58-âĂŞ66 (2006).
7. A. Biberman, S. Manipatruni, N. Ophir, L. Chen, M. Lipson, and K. Bergman, "First demonstration of long-haul transmission using silicon microring modulators," Opt. Express **18**, 15544-âĂŞ15552 (2010).
8. S. Xiao, M. H. Khan, H. Shen, and M. Qi, "Compact silicon microring resonators with ultra-low propagation loss in the C band," Opt. Express **15**, 14467–14475 (2007).
9. V. P. Heuring, "Bit-serial architecture for optical computing D = AC + BC," Appl. Opt. **31**, 3213–3224 (1992).
10. K. De Vos, I. Bartolozzi, E. Schacht, P. Bienstman, and R. Baets, "Silicon-on-Insulator microring resonator for sensitive and label-free biosensing," Opt. Express **15**, 7610–7615 (2007).
11. J. L. OâĂŹBrien, G. J. Pryde, A. G. White, T. C. Ralph, and D. Branning, "Demonstration of an all-optical quantum controlled-NOT gate," Nature **426**, 264–267 (2003).
12. J. W. Silverstone, D. Bonneau, K. Ohira, N. Suzuki, H. Yoshida, N. Iizuka, M. Ezaki, C. M. Natarajan, M. G. Tanner, R. H. Hadfield, V. Zwiller, G. D. Marshall, J. G. Rarity, J. L. OâĂŹBrien, and M. G. Thompson, "On-chip quantum interference between silicon photon-pair sources," Nat. Photonics **8**, 104–108 (2013).
13. A. Politi, J. Matthews, M. G. Thompson, and J. L. OâĂŹBrien, "Integrated Quantum Photonics," IEEE J. Sel. Top. Quantum Electron. **15**, 1673–1684 (2009).
14. P. Orlandi, F. Morichetti, M. J. Strain, M. Sorel, P. Bassi, and A. Melloni, "Photonic integrated filter with widely tunable bandwidth," IEEE J. Lightwave Technol. **32**, 897–907 (2014).
15. S. Ristic, "An Optical Phase-Locked Loop Photonic Integrated Circuit," IEEE J. Lightwave Technol. **28**, 526–538 (2010).
16. A. Huang, C. Gunn, L. Guo-Liang, L. Yi, S. Mirsaidi, A. Narasimha, and T. Pinguet, " A 10Gb/s photonic modulator and WDM MUX/DEMUX integrated with electronics in 0.13 μm SOI CMOS," in Proceedings of the Solid-State Circuits Conference Digest of Technical Papers (2006), pp. 922–929.

#294678 https://doi.org/10.1364/OE.25.019711
Journal © 2017 Received 1 May 2017; revised 31 Jul 2017; accepted 31 Jul 2017; published 7 Aug 2017

Optics EXPRESS

17. K. De Vos, J. Girones, T. Claes, Y. De Koninck, S. Popelka, E. Schacht, R. Baets, and P. Bienstman, "Multiplexed antibody detection with an array of silicon-on-insulator microring resonators," IEEE Photon. J. **1**, 225–235 (2009).
18. D. Grassani, S. Azzini, M. Liscidini, M. Galli, M. J. Strain, M. Sorel, J. E. Sipe, and D. Bajoni, "Micrometer-scale integrated silicon source of time-energy entangled photons," Optica **2**, 88–94 (2015).
19. N. C. Harris, D. Grassani, A. Simbula, M. Pant, M. Galli, T. Baehr-jones, M. Hochberg, D. Englund, D. Bajoni, and C. Galland, "Integrated Source of Spectrally Filtered Correlated Photons for Large-Scale Quantum Photonic Systems," Phys. Rev. X **4**, 041047 (2014).
20. C. Reimer, M. Kues, P. Roztocki, B. Wetzel, F. Grazioso, B. E. Little, S. T. Chu, T. Johnston, Y. Bromberg, L. Caspani, D. J. Moss, and R. Morandotti, "Generation of multiphoton entangled quantum states by means of integrated frequency combs," Science **351**, 6278 (2016).
21. P. Dong, N.-N. Feng, D. Feng, W. Qian, H. Liang, D. C. Lee, B. J. Luff, T. Banwell, a Agarwal, P. Toliver, R. Menendez, T. K. Woodward, and M. Asghari, "GHz-bandwidth optical filters based on high-order silicon ring resonators," Opt. Express **18**, 23784–23789 (2010).
22. X. Wang, W. Shi, S. Grist, H. Yun, N. A. F. Jaeger, and L. Chrostowski, "Narrow-band transmission filter using phase-shifted Bragg gratings in SOI waveguide," IEEE Photonics Conf. (Arlington, VA) paper ThZ1 (2011).
23. X. Wang, S. Grist, J. Flueckiger, N. A. F. Jaeger, and L. Chrostowski, "Silicon photonic slot waveguide Bragg gratings and resonators," Opt. Express **21**, 19029 (2013).
24. T. Liow, M. Yu, and G. Lo, "Silicon High-Order Coupled-Microring-Based Optical Interconnects," IEEE Photon. Technol. Lett. **24**, 821-âĂŞ823 (2012).
25. J. R. Ong, R. Kumar, and S. Mookherjea, "Silicon microring-based wavelength converter with integrated pump and signal suppression," Opt. Lett. **39**, 4439-âĂŞ4441 (2014).
26. J. R. Ong, R. Kumar, and S. Mookherjea, "Ultra-High-Contrast and Tunable-Bandwidth Filter Using Cascaded High-Order Silicon Microring Filters," IEEE Photon. Technol. Lett. **25**, 1543-âĂŞ1546 (2013).
27. F. Morichetti, A. Canciamilla, C. Ferrari, M. Torregiani, A. Melloni, and M. Martinelli, "Roughness induced backscattering in optical silicon waveguides," Phys. Rev. Lett. **104**, 33902 (2010).
28. D. Hofstetter and R. L. Thornton, "Theory of loss measurements of Fabry Perot resonators by Fourier analysis of the transmission spectra," Opt. Lett. **22**, 1831–1833 (1997).
29. J. Poon, J. Scheuer, S. Mookherjea, G. Paloczi, Y. Huang, and A. Yariv, "Matrix analysis of microring coupled-resonator optical waveguides," Opt. Express **12**, 90–103 (2004).
30. F. Morichetti, A. Canciamilla, C. Ferrari, A. Samarelli, M. Sorel, and A. Melloni, "Travelling-wave resonant four-wave mixing breaks the limits of cavity-enhanced all-optical wavelength conversion," Nat. Commun. **2**, 296 (2011).
31. X. Sun, M. Z. Alam, S. J. Wagner, J. S. Aitchison, and M. Mojahedi, "Experimental demonstration of a hybrid plasmonic transverse electric pass polarizer for a silicon-on-insulator platform," Opt. Lett. **37**, 4814–4816 (2012).
32. P. Orlandi, F. Morichetti, M. J. Strain, M. Sorel, A. Melloni, and P. Bassi, "Tunable silicon photonics directional coupler driven by a transverse temperature gradient," Opt. Lett. **38**, 863–865 (2013).
33. A. C. Turner, M. A Foster, A. L. Gaeta, and M. Lipson, "Ultra-low power parametric frequency conversion in a silicon microring resonator," Opt. Express **16**, 4881-âĂŞ4887 (2008).
34. M. J. Strain, C. Lacava, L. Merrigi, I. Cristiani, and M. Sorel, "Tunable Q-factor silicon micro-ring resonators for ultra-low power parametric processes," Opt. Lett. **40**, 1274–1277 (2014).

1. Introduction

Silicon on insulator (SOI) is one of the most mature and well developed photonic integration platforms [1–5], benefiting from the availability of CMOS fabrication technology, where it is possible to use electronics fabrication facilities to make photonic circuitry [6]. The large refractive index contrast between the two materials allows a strong confinement of the optical mode to waveguide cross-sections with sub-micron dimensions, making SOI photonics an interesting technology for application in telecommunications [7–9], biosensing [10] and quantum optics [11–13].

Photonic filters are one of the key elements in optical communication systems [14] and have attracted significant interest due to their potential for a wide range of applications, including noise suppression [15], signal quality improvement, on-chip networking [16], spectroscopy [17] and pump filtering for non-linear optics [18]. Most of these applications require modest filter extinction ratios in the order of $20 - 30$ dB. However, in some applications, such as on-chip sources for correlated photon pair generation, filters with much higher extinction ratios for the on-chip pump are required [19, 20].

On-chip silicon photonic filters optimised for TE polarisation have been demonstrated with

Optics EXPRESS

high quality factors and extinction values ≈ 45-50 dB [21–25]. High extinction values (≈ 100 dB) have been reached in a few cases, using a grating filter coupled with two ring resonators [19] or using two 5^{th} order CROW (coupled resonator optical waveguide) filters on separate chips [26].

Critically however, devices optimised for TE mode filtering do not inherently suppress light propagating in the orthogonal TM polarisation. This becomes a significant issue in silicon photonics where scattering between the TE and TM modes has been shown to be non-negligible in typical SOI waveguides (220nm × 500nm) fabricated by reactive ion etching, limiting polarisation extinction to ≈ 20 dB [27]. This effect therefore leads to the potential for a significant amount of light to be scattered from the TE to the TM mode in access waveguides then transmitted through the TE mode filter.

In this work a filter design acting on both TE and TM polarisation components is presented. The TE light is filtered using a cascade of ring resonator devices. Due to birefringence of the TE and TM modes, the cascaded rings present TM mode passbands within the TE stopbands. To attenuate the TM modes a metal layer is fabricated over the ring. In section 2 the design, technology and the linear response the filter is presented. The effects of polarisation mode scattering on high extinction filters is shown in section 3. In section 4 the performance of the fabricated filter is demonstrated. Section 5 presents application of these filters in non-linear Four Wave Mixing generation and filtering fully on-chip. Conclusions are given in section 6.

2. Device technology

The SOI waveguides investigated in this work consist of a silicon core with height of 220 nm and width of 500 nm, primarily designed for TE optimised PICs. The waveguide device patterning was defined using electron beam lithography with Hydrogen Silsequioxane (HSQ) as the resist layer, which was transferred to the silicon core by Reactive Ion Etching. In order to increase the coupling efficiency inverse tapers and polymer waveguides were used to couple the light in and out of the chip. The polymer waveguides were fabricated in SU8, with dimensions of 5 μm in width and 3.5 μm in height. The silicon waveguides were coated with a 1 μm thick plasma enhanced chemical vapour deposition (PECVD) SiO_2 as a buffer layer. In this work the ring resonator devices were realised as racetrack geometries to allow control over the bus waveguide to ring coupling fraction. Any reference to ring resonators refer to this racetrack geometry. An example Scanning Electron Microscope (SEM) image of a racetrack resonator device is shown in Fig. 1.

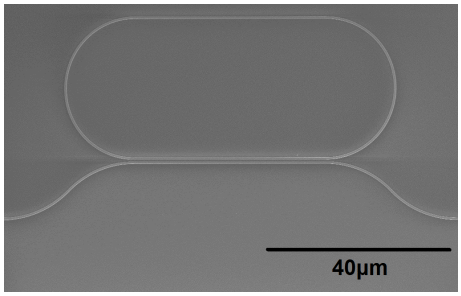

Fig. 1. SEM image of a single all pass ring resonator.

The transmission spectra of the filters were measured by coupling light, using polarisation maintaining fibre (PM), from a tunable CW laser through a fiber polarisation filter, with an extinction ratio of 20 dB aligned with the TE mode, to a PM lensed fibre and input polymer waveguide. The output light was coupled into a second PM lensed fibre and the output signal was sent to an optical spectrum analyser (OSA). No polarisation selective off-chip filters were applied

Optics EXPRESS

after transmission through the chip. The polarisation extinction before the chip was measured at 20 dB.

Loss measurements for SOI straight waveguides co-fabricated with the filters were carried out using a Fabry-Perot technique to extract the propagation loss values [28] . Average propagation losses of 0.5 dBcm^{-1} and 5 dBcm^{-1} were measured for TE and TM modes respectively. Fiber to polymer inverse taper losses were measured at 2.5 dB per facet.

3. Polarisation effects in ring resonator filters

High extinction filters based on ring resonator devices have been demonstrated using a coupled-resonator optical waveguide (CROW) geometry [26]. Here we present an alternative cascade of ring resonators, both are shown schematically in Fig.2. In both CROW and cascade geometries, the number of resonators can be increased in order to increase the filter rejection but, given the sensitivity of the OSA detection system and the substrate light noise, described in section 5, the number of the rings used in this work has been limited to three.

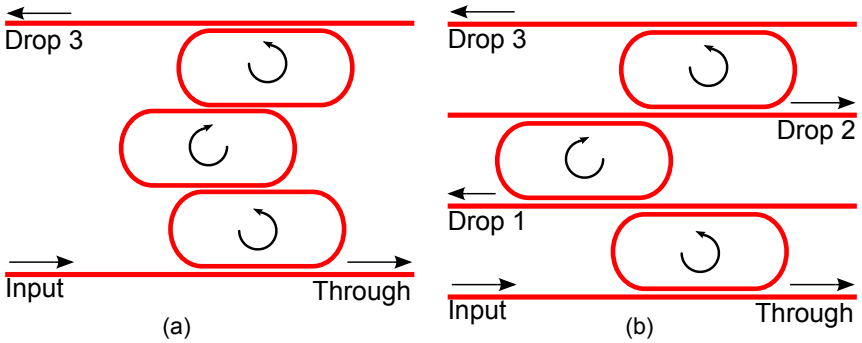

Fig. 2. Schematics of third order (a) CROW and (b) Cascaded ring filter geometries.

Simulated transmission spectra for each filter for TE transmission are presented in Fig. 3. The simulations are obtained using a Transfer Matrix Method (TMM) model of a ring resonator [29] and consider resonators with a straight waveguide section length of 42 μm and bend radius of 15 μm. All couplers are designed to produce a power coupling coefficient of 0.1 for the TE mode, by lateral offset of the bus and racetrack straight waveguide sections, where the coupler gap is 300 nm. Propagation losses are set at 0.5 dBcm^{-1} and the coupler section introduces a point loss of 0.05 dB. The simulation also takes into account constant insertion losses of the fiber to chip coupling of 5 dB from experimental results. The calculated Q-factor of a single add-drop ring operating in the TE polarisation is calculated as 11.7 k. Similarly, with values of coupling coefficient and propagation loss equal to 0.14 and 5 dBcm^{-1}, respectively, for the TM polarisation in the same ring device, a Q-factor of 6.7 k is calculated. Figure 3(b) shows how the cascade, being a set of first order filters, presents the notch corresponding to the transmission of the next ring at each output. i.e. the drop signal after two rings (Drop 2) presents a notch relative to the transmission of the third ring. This allows tuning of the transmission of the third ring with the drop peak of the second.

The CROW is effectively a third order filter, whereas the cascade is a series of three first order filters. This produces a bandwidth of $\approx$ 650 pm in the CROW case, and $\approx$ 70 pm for the cascade, and a maximum extinction ratio, calculated to be 20 dB higher in the cascade case. In this work we will focus on the narrow band and high rejection, cascade filters.

Figure 4(a) shows the simulated transmission for both ideal TE and TM injection. These simulations were carried out using the TMM model with the relevant polarisation mode parameters detailed above. Therefore if the major polarisation is TE, a -20 dB scattering can couple to the

Optics EXPRESS

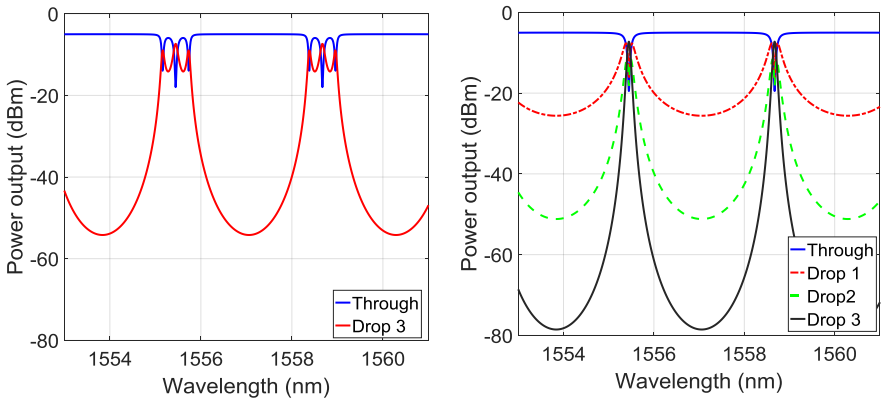

Fig. 3. Simulated TE mode spectra of (a) CROW and (b) cascaded ring filters, calculated for the through and drop port outputs.

TM mode in the waveguide. This means that, on resonance, the -20 dB light scattered into the TM mode will be transmitted in the extinction bands of the TE filter response [30]. Since the effective refractive index for the two polarisation modes is different, a significant amount of TM light is therefore predicted in the TE rejection band.

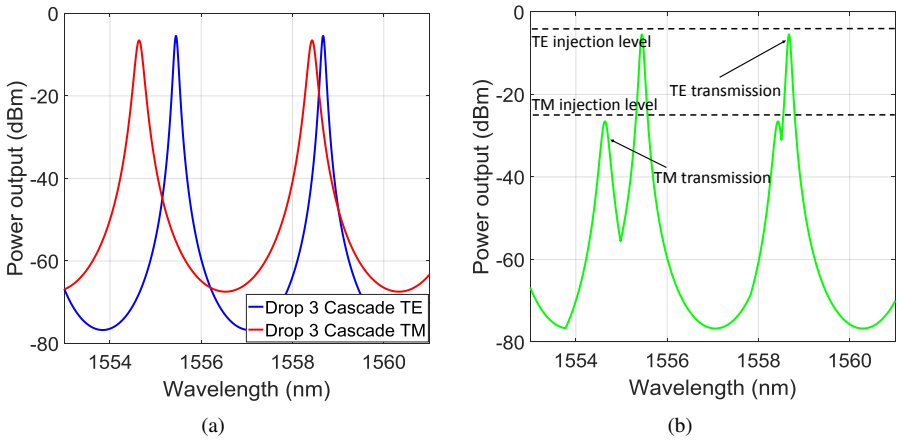

Fig. 4. (a) Comparison of simulated linear transmission between ideal TE and TM injection for a three ring cascade device. (b) Simulated transmission spectra of a three ring cascade filter for both polarisations, including 20dB input polarisation extinction ratio.

Figure 4(b) shows a TMM transmission spectrum simulation of a device where the TE to TM mode injection ratio is 20dB. The significant amount of TM light predicted in the TE filter stopbands highlights the requirement for TM mode filtering on-chip.

4. Plasmonic TM mode attenuator

As detailed above, in filters designed for TE applications, significant levels of TM polarised light can be transmitted. It is therefore necessary, to suppress the TM in addition to the TE. In Fig. 5 a cross section of a TE and a TM mode in a SOI waveguide is shown. The TE mode, Fig. 5(a), is

Optics EXPRESS

concentrated in the high index region (i.e. silicon core) while the TM mode, shown in Fig. 5(b), shows a higher fraction of the mode energy propagating in the lower index region (i.e. silica).

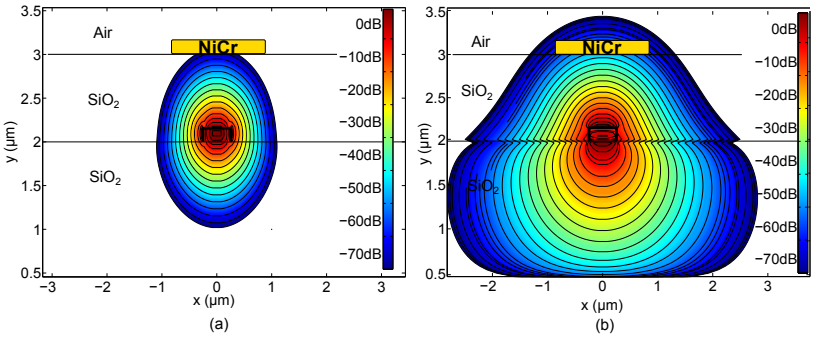

Fig. 5. Mode cross section for TE (left) and TM (right) polarised field in a 220 × 500 *nm* SOI waveguide.

By placing an additional metal layer on top of the device, as demonstrated in previous studies [31], it is possible to attenuate the TM without affecting the TE mode propagation. This because the large TM field overlap with the metal enhances the TM losses but not the more confined TE. Based on this principle, a filter suppressing both TE and TM mode components can be implemented by fabricating the metal layer on a TE filter design.

A set of straight waveguides were fabricated with the length of metal cladding above the guide as a parameter. This set of devices provided an equivalent to the cutback loss measurement technique for the plasmonic attenuator. Measurements of the TE mode propagation show no measurable change of losses between cases where the metal is present or not. Losses are measured at around 0.5 dBcm^{-1} in both cases. In the case of TM mode propagation, the loss (shown in Fig. 6) is found to be around 60 dBcm^{-1} at 1550 nm, compared to the 5 dBcm^{-1} for waveguides fabricated without metal. This solution is particularly straightforward to implement in the tunable filter design presented here.

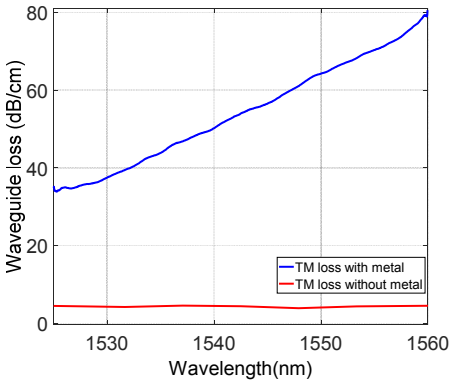

Fig. 6. Measured waveguide loss as a function of the input wavelength for a TM injection in a single waveguide with NiCr cross sectional area of 50 × 900 nm.

All of the ring resonators used in this work have NiCr heating elements fabricated above the ring waveguide cross section. This is in order to obtain the necessary resonance wavelength tunability, as shown in [32]. This heating element then provides not only the tunability function but also the necessary TM plasmonic absorption losses. Furthermore, although the TM absorption

Optics EXPRESS

is only a few tens of $dBcm^{-1}$, the resonant enhancement of the TM mode on-resonance with the ring, provides significant loss over the relatively short path length of the resonator.

Figure 7(a) shows the measured output after three stages of the 3 ring cascade device, comparing this result with the simulation first shown in Fig. 3(b). Injecting TE polarised light, with a TM component at -20 dB, the device filters both polarisation components with only 1.8 dB of insertion loss on the TE mode. The results present an excellent match with the simulation of a 3 ring cascade with the same parameters as the one tested.

In Fig. 7(b) a measurement of the transmission spectrum at the Drop 3 port is shown for TM injection. Changing the injection light to a TM polarisation, the TE polarised light component is now injected at -20 dB (i.e. the inverse case of Fig. 7(a)).

In this measurement the TM propagation shows an excess loss due to the plasmonic filter of 50 dB. Therefore, in a TE injection measurement, Fig. 7(a), where the TM polarised field was injected with -20 dB with respect to the TE, the TM component is filtered to below the noise floor of the measurement. The low loss of the TE component is shown in 7(b) where a strong TE signal at -27 dBm is measured.

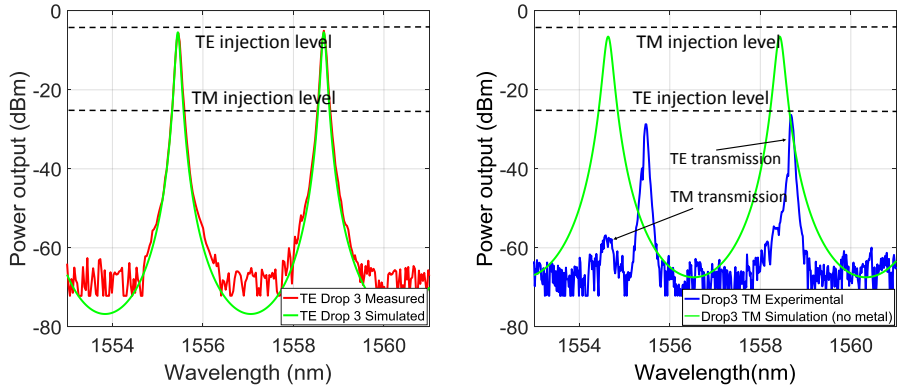

Fig. 7. Drop 3 port transmission measurements of a cascade device for (a) TE and (b) TM, dominant injection modes (ER 20dB)

5. Monolithic device for FWM and on-chip pump filtering

In order to demonstrate the capabilities allowed by full on-chip filtering of both polarisations, the 3 ring cascade filter detailed above was monolithically integrated with another ring resonator device for generation of FWM signals [33, 34]. The FWM generation device (or source ring) was designed to be exactly twice the optical path length of the rings constituting the cascaded ring filter. In this way the FSR of the source ring is exactly half that of the filter, and therefore the filter can selectively pass the pump wavelength to the through port, while the adjacent resonances carry the signal and idler beams to the drop port. The schematic of the device is presented in Fig. 8.

The experimental setup used, shown in Fig.9, is similar to the one described in the previous section, with the addition of two polarisation controls and a 3 dB coupler, but, as before, no polarisation selective off-chip filters have been applied after transmission through the chip. Measurements were taken at: 'T1' the through port of the filter when it was detuned from the source ring modes, 'T2' the through port of the filter when on-resonance with the source ring modes, and 'D3' the Drop 3 port of the filter on-resonance with the source ring.

Optics EXPRESS

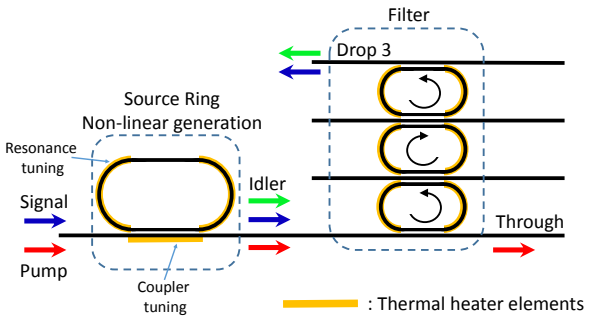

Fig. 8. A schematic of the monolithically integrated four-wave mixing source with cascade ring filter.

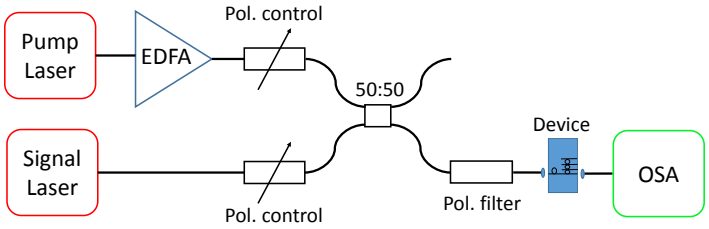

Fig. 9. Experimental setup used for non-linear measurements on the monolithic device.

First, in order to characterise the FWM efficiency of the source ring, the source ring resonances were detuned from the filter resonances. The FWM efficiency was calculated following [33], with the FWM efficiency defined as: $(10log_{10}(P_i/P_s))$, where P_i is the measured idler power and P_s is the input signal power. The on-chip pump and signal powers (measured in the absence of one another) were measured by detuning the relevant line from the source ring resonances. In this work the on-chip pump power was 2 mW and the signal power was 0.01 mW. The idler output power was measured at the output of the chip. The source ring coupling coefficient was tuned to the critical coupling point to provide the best FWM efficiency. The peak FWM efficiency measured was −22 dB at a coupling coefficient value of 5 %, corresponding to a source ring Q-factor of 30 k. Figure 10(a) shows the measured FWM spectra at the filter through port. Since the source ring is in series with the cascaded ring filter, the measured spectra include the effects of both devices. Therefore the T1 and T2 curves show the main pump peak and background ASE light measured by the OSA. In the T1 curve the notches in the ASE background are due to the cascade rings filtering the input light to the chip.

The source ring and three rings of the cascaded filter were then aligned in wavelength using thermal heating elements above each ring, making use of the intermediate drop ports of the filter to ensure optimal alignment of each stage. The through port transmission, T2, in this case is shown in Fig.10(a). Since the pump light is aligned with a source ring resonance between two of the filter resonance lines, it was then possible, as shown in Fig. 10(b), to transmit the signal and the generated idler to the Drop 3 output. The residual pump light transmitted through the Drop 3 port is reduced down to the substrate scattering noise level of our system. The transmitted signal and idler show insertion losses of 1.8 dB, matching the linear transmission measurements.

The peak appearing around 1557 nm in the D3 curve of Fig. 10(b) is not limited by waveguide transmitted pump light but rather by scattered light in the device substrate. Figure 11(a) shows how this measured residual pump signal is related to the distance of the output fibre from the

Optics EXPRESS

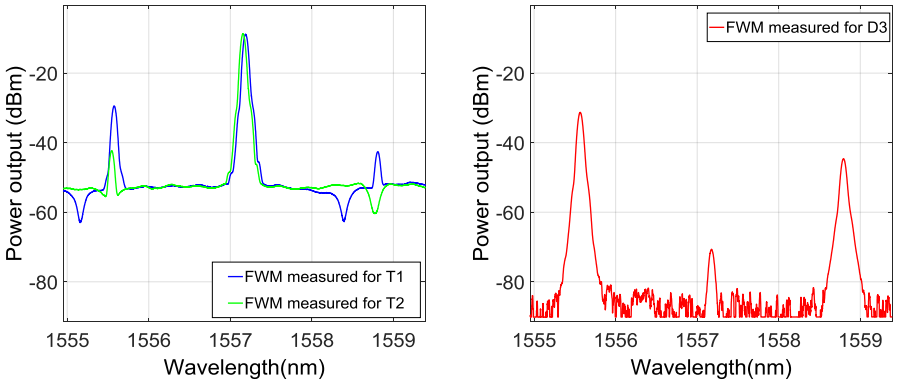

(a) (b)

Fig. 10. (a) Four wave mixing signals measured at the filter through port. T1 shows the FWM at the through port with the source ring off resonance with the filter. T2 shows the through port with the source ring on resonance with the filter. (b) Four wave mixing signals measured at the filter Drop 3 port, D3, with the source ring on resonance with the filter.

filter's output waveguide. To decrease the measured signal level by 10 dB it is necessary to move the output fibre 1 mm away from the output waveguide. This can be compared with the calculated modal overlap between the SU8 waveguide and tapered fibre modes using a finite element mode solver. As shown in Fig.11(b), the modal coupling is expected to rapidly decrease with micron scale misalignment, confirming that the measured signal is not due to light guided in the waveguide.

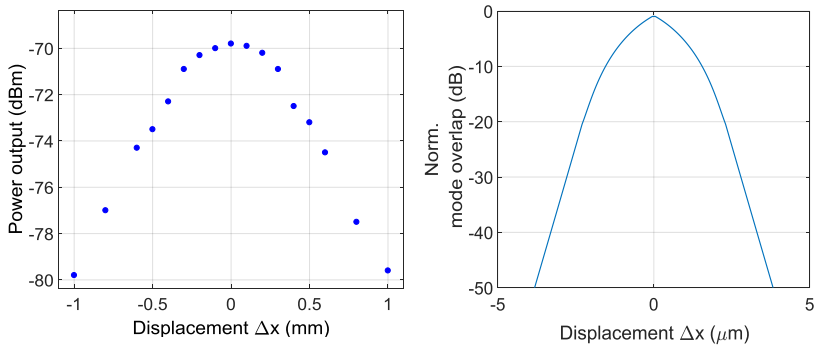

(a) (b)

Fig. 11. (a) Substrate light scattering captured by the output lensed fibre as a function of the displacement from the output filter's waveguide. (b) Calculated modal overlap between waveguide and fibre modes as a function of lateral displacement.

6. Conclusion

In conclusion, a filter consisting of elements to filter both TE and TM polarisations was demonstrated. The primary filter is based on a cascade of ring resonator devices operating on the TE polarisation. Residual TM light in the filter stopbands is apparent due to the birefringent nature

Optics EXPRESS

of the device. In order to filter the TM mode, a metallic layer was fabricated above the upper cladding of the ring filter, making use of resonantly enhanced TM mode losses. This metal layer also acted as a thermal tuning element for the ring filter. The filter exhibits a high total extinction ratio of over 60 dB obtained for both TE and TM transmitted modes, for an input TE:TM extinction ratio of 20 dB. The filter rejection can be increased by adding more rings to the cascade, but was limited here by the dynamic range of the measurement system and substrate scattered light. Finally, by integrating the ring resonator filter technology with a further ring resonator device for non-linear optical generation, FWM experiments were carried out obtaining an on-chip pump extinction of 62 dB and insertion loss of signal and idler of 1.8 dB.

Funding

Engineering and Physical Sciences Research Council (EPSRC) (EP/L021129/1); EU FP-7 (323734).

Acknowledgments

The authors wish to thank the staff of the James Watt Nanofabrication Centre at the University of Glasgow. G.C. acknowledges studentship support from the Fraunhofer Centre for Applied Photonics.

130.209.115.202 {ts '2017-09-01 05:17:27'}